



**HAL**  
open science

# Impact of oxidation and biodegradation on the most commonly used polycyclic aromatic hydrocarbon (PAH) diagnostic ratios: Implications for the source identifications

Coralie Biache, Laurence Mansuy-Huault, Pierre Faure,

## ► To cite this version:

Coralie Biache, Laurence Mansuy-Huault, Pierre Faure,. Impact of oxidation and biodegradation on the most commonly used polycyclic aromatic hydrocarbon (PAH) diagnostic ratios: Implications for the source identifications. *Journal of Hazardous Materials*, 2014, 267, pp.31-39. 10.1016/j.jhazmat.2013.12.036 . hal-01076256

**HAL Id: hal-01076256**

**<https://hal.science/hal-01076256>**

Submitted on 29 Jan 2018

**HAL** is a multi-disciplinary open access archive for the deposit and dissemination of scientific research documents, whether they are published or not. The documents may come from teaching and research institutions in France or abroad, or from public or private research centers.

L'archive ouverte pluridisciplinaire **HAL**, est destinée au dépôt et à la diffusion de documents scientifiques de niveau recherche, publiés ou non, émanant des établissements d'enseignement et de recherche français ou étrangers, des laboratoires publics ou privés.

# Impact of oxidation and biodegradation on the most commonly used polycyclic aromatic hydrocarbon (PAH) diagnostic ratios: Implications for the source identifications

*Coralie Biache<sup>a,b,\*</sup>, Laurence Mansuy-Huault<sup>a,b</sup>, Pierre Faure<sup>a,b</sup>*

<sup>a</sup> University of Lorraine, LIEC, UMR7360, Vandoeuvre-lès-Nancy F-54506, France

<sup>b</sup> CNRS, LIEC, UMR7360, Vandoeuvre-lès-Nancy F-54506, France

\* Corresponding author at: LIEC, Faculty of Sciences and Technology, Boulevard des Aiguillettes, B.P. 70239, 54506 Vandoeuvre-lès-Nancy Cedex, France.

Tel.: +33 3 83 68 47 40.

E-mail address: coralie.biache@yahoo.fr (C. Biache).

## Highlights

- Impact of degradation processes on PAH ratios in coking plant soil was studied.
- Biodegradation and abiotic oxidation experiments were performed.
- Ratios involving low molecular weight PAHs were particularly affected.
- Biodegradation induced a shift in the PAH ratios toward combustion signature.
- Abiotic oxidation caused a change in the PAH ratios toward petrogenic signature.

Keywords: PAH; Diagnostic ratio; Oxidation; Biodegradation; Coking plant soil

## Abstract

Based on the isomer stability during their formation, PAH diagnostic ratios have been extensively used to determine PAH contamination origin. Nevertheless, it is known that these isomers do not present the same physicochemical properties and that reactions occurring during the transport from an atmospheric source induce changes in the diagnostic ratios. Yet, little is known about reactions occurring in soils contaminated by other sources such as coal tar and coal. Innovative batch experiments of abiotic oxidation and microbial incubations were performed to discriminate independently the influence of these two major processes occurring in soils on the diagnostic ratios of major PAH sources. Three samples were studied, a coking plant soil and two major PAH sources in this soil, namely coal and coal tar. The combustion signature of the coking plant soil showed the major influence of coal tar in the soil sample composition. Some of these ratios were drastically affected by oxidation and biodegradation processes inducing a change in the source signature. The coal tar signature changed to petrogenic source after oxidation with the anthracene/(anthracene + phenanthrene) ratio. According to this ratio, the initial petrogenic signature of the coal changed to a combustion signature after the biodegradation experiment.

## 1. Introduction

The polycyclic aromatic hydrocarbons (PAHs) are a class of several hundreds of compounds, formed with at least two fused benzene rings. Overall, two major processes can result in their formation. They are produced by the incomplete combustion of organic matter (OM) such as biomass, coal and oil, and other high temperature processes such as coking [1] and also occur during OM diagenesis and can be consequently found in diagenetically transformed OM (coal, crude oil) and refined petroleum products [2]. Finally, they can be biosynthesized by some plants and fungi [3] in superficial environment, but this last source represents only a small proportion of PAHs released in the environment. Most of them originate from anthropogenic inputs, related to the exploitation, transformation and combustion of fuels [4]. PAHs received a particular attention for the last decades because of their toxic, mutagenic and carcinogenic properties, and for their persistence in the environment explaining why 16 PAHs are listed as priority pollutants by the USEPA (United States Environmental Protection Agency) [5]. They are also used as tracers of anthropogenic activities in continental sediments or terrigenous organic carbon in marine sediments [6]. Considering the ubiquitous presence of the PAHs in the environment and the health risks related to their exposure, it became necessary to identify the discharge points. PAH diagnostic ratios (Table 1) are often used to discriminate the contamination sources [7–13]. They mainly allow distinguishing between petroleum and combustion contributions whereas some ratios refine the determination between fuel combustion, coal combustion and wood combustion. These calculations are based on the relative thermodynamic stability of some PAH isomers. The isomers called “kinetic”, formed from rapid reactions and presenting a low relative stability [11], are mainly generated during combustion processes or thermal treatments. The “thermodynamical” isomers present higher relative stability and are produced during long time processes such as diagenesis or catagenesis [11]. As a result, fossil OM, such as crude oil or coal, defined as petrogenic sources are enriched in the “thermodynamical” isomers. Fossil OM is also enriched in alkylated (Alk) PAHs compared to OM originating from combustion which contains more parent (Par) PAHs, also allowing to use  $\text{Par}/(\text{Par} + \text{Alk})$  as a diagnostic ratio.

**Table 1:** PAH diagnostic ratios and their significations. (a): Yunker et al. [11] and references therein, (b): Yan et al. [7] and references therein. Abbreviations: sum of An and Phe/sum of An, Phe and their methylated counterparts (CO/(CO + C1)178), sum of Fl and Py/sum of Fl, Py and their methylated counterparts (CO/(CO + C1)202), sum of the parent PAHs with m/z 128, 178, 202 and 228/sum of these parent PAHs and their alkylated counterparts (Par/(Par + Alk)), sum of the 4, 5 and 6 ring PAHs/sum of the total PAHs (456 Ring/TPAH), 1,7-dimethylphenanthrene/(1,7-dimethylphenanthrene + 2,6-dimethylphenanthrene) (1,7/(1,7 + 2,6) DMP)). See Table 2 for compound name abbreviations.

| Diagnostic ratios    | Petrogenic | Petroleum burning | Coal combustion | Softwood combustion | References |
|----------------------|------------|-------------------|-----------------|---------------------|------------|
| Ant/(Ant + Phe)      | < 0.10     | > 0.10            | > 0.10          | > 0.10              | a,b        |
| Flu/(Flu + Py)       | < 0.40     | 0.40 - 0.50       | > 0.50          | > 0.50              | a, b       |
| B(a)A/(B(a)A + Chry) | < 0.20     | > 0.35            | > 0.35          | > 0.35              | a, b       |
| CO/(CO + C1)178      | < 0.50     | > 0.50            | > 0.50          | > 0.50              | a, b       |
| CO/(CO + C1)202      | < 0.50     | > 0.50            | > 0.50          | > 0.50              | a, b       |
| IP/(IP + B(ghi)P)    | < 0.20     | 0.20-0.50         | > 0.50          | > 0.50              | a, b       |
| Par/(Par + Alk)      | < 0.30     | > 0.50            | > 0.50          | > 0.50              | b          |
| Ring 456/TPAH        | < 0.40     | > 0.50            | > 0.50          | > 0.50              | b          |
| 1,7/(1,7 + 2,6)DMP   | /          | < 0.45            | > 0.70          | > 0.70              | a          |

The use of these ratios is based on the hypothesis that PAH isomers present the same physico-chemical properties and will consequently be transformed and degraded at the same rate, preserving the ratio values of the emission source(s). However, there are differences in water solubility and volatility between two PAHs of the same molecular weight (Table 2) that can be responsible for a higher transformation/degradation rate for one of the isomers inducing a change in the diagnostic ratio. This question has already been raised by several authors [14–17]. Kim et al. [18] studied the loss rate of soot-associated PAHs under controlled laboratory conditions of temperature and irradiation and observed changes in the PAH diagnostic ratios after irradiation with a shift of the Fluoranthene/(Fluoranthene + Pyrene) (Fl/(Fl + Py)) ratio from gasoline combustion toward diesel combustion and a change from pyrogenic to petrogenic source with the (Benzo[a]anthracene/(Benzo[a]anthracene + Chrysene) (B(a)A/(B(a)A + Chry)) ratio. Zhang et al. [13] showed that PAHs present different rate of transformation during their transport in a multimedia environment causing a change in their diagnostic ratios and they proposed a correction of the PAH diagnostic ratios based on a multimedia model under specific site conditions. These studies mainly focus on reactions occurring during the transport of PAHs from atmospheric sources, principally photodegradation or partitioning between gas and particle phases, yet little is known about reactions occurring in the soils or sediments containing PAH-rich organic constituents (i.e. coal, coal tar). These

constituents can be transported through water-washing in different media such as aquatic sediments, sewage deposit or wastewater sludge where the origin of the contamination also needs to be determined. Moreover, no data are available regarding the influence of individual processes such as oxidation and biodegradation occurring in soils.

The objectives of this study were (i) to identify the changes in the PAH diagnostic ratios occurring independently during two major processes taking place during natural attenuation, i.e. abiotic oxidation and biodegradation, of a coking plant soil and its major organic constituents and (ii) to identify ratio(s) preserving the source signature in order to determine the more reliable parameters in the source identification. In order to fulfill these objectives, innovative batch experiments were designed. Abiotic oxidation and biodegradation experiments were performed for 180 days and 270 days, respectively, on a coking plant soil as well as on coal and coal tar which are major organic constituents of a coking plant soil and constitute major PAH sources. The impact of abiotic oxidation and biodegradation on the soil OM, (more particularly on the extractable OM) was already studied and published [19,20]. For the present study, PAHs were quantified with gas chromatography–mass spectrometry (GC-MS), and several diagnostic ratios were calculated before and after the experiments.

## **2. Experimental**

### *2.1. Samples and sample preparation*

Samples used in the oxidation and biodegradation experiments were a coal tar (from the Marienau Pyrolysis Center, France), and a type III coal (Merlebach, France). The coking plant soil was sampled in a former coking plant site in Homécourt (Lorraine, France). The physico-chemical parameters of the coking plant soil are described elsewhere [21]. Another coal tar was also sampled in a soil cavity containing coal tar in the same site (Homécourt). Since this sample is inherited from the coking plant activities which ended in the 80 s, this sample will be referred as “aged” coal tar.

Coal sample was crushed to come through a 40 µm mesh sieve and the coking plant soil sample was crushed to pass through a 500 µm mesh sieve. The coal tar was previously spread out on silica (4% of coal tar) in order to increase the surface contact with air oxygen.

## *2.2. Batch experiments*

### *2.2.1. Abiotic oxidation*

The oxidation experiment was described elsewhere [20]. Briefly, 15 g of each sample, except the “aged” coal tar, were introduced into closed 100 mL Schott bottles. Two repetitions of each sample were placed into an oven at 100 °C for 180 days. Working at such temperature for such a long time prevented microorganisms to develop and biodegradation to occur simultaneously. Every 15 days, the bottles were cooled at ambient temperature and opened to renew the flask atmosphere (especially air oxygen). After the oxidation time, samples were stored at –18 °C before analysis.

### *2.2.2. Biodegradation*

The incubation experiment was described elsewhere [19]. Briefly, for each sample except the “aged” coal tar, three replicates of 25 g were put into 250 mL Schott bottles. A microbial inoculum of the Homécourt coking plant soil sample was prepared by adding to 1 g of soil, 6 g of glass beads and 10 mL of NaCl 0.85% solution and shaking the mixture for 1 h. One milliliter of this mixture as well as 30 mL of a mineral nutritive solution (Bushnell Haas, 3.27 g L<sup>-1</sup>) was added to the samples. The bottles were hermetically closed and placed into an incubation chamber at 24 °C in the dark and were continuously stirred. Triplicates of samples were harvested after 270 days. As discussed in Biache et al. [19], considering the impossibility to maintain the media sterile for this duration [22,23], no sterile control samples were used in this study. The bottles were regularly opened (every other days during the first 18th days of the experiment and then spaced out every 15 days) to renew the atmosphere. After the incubation period, samples dedicated to PAH quantification were freeze-dried and stored at –18 °C.

**Table 2:** PAHs used for the diagnostic ratios with their abbreviations and some of their physico-chemical properties.

| Compound                        | Abbreviation | Number of rings | Molecular weight g mole <sup>-1</sup> | Water solubility (g m <sup>-3</sup> ) | log(Kow) |
|---------------------------------|--------------|-----------------|---------------------------------------|---------------------------------------|----------|
| Phenanthrene                    | Phe          | 3               | 178                                   | 1.1                                   | 4.57     |
| Anthracene                      | An           | 3               | 178                                   | 0.045                                 | 4.54     |
| Fluoranthene                    | Flu          | 4               | 202                                   | 0.26                                  | 5.22     |
| Pyrene                          | Py           | 4               | 202                                   | 0.13                                  | 5.18     |
| Benzo[ <i>a</i> ]anthracene     | B(a)A        | 4               | 228                                   | 0.011                                 | 5.91     |
| Chrysene                        | Chry         | 4               | 228                                   | 0.006                                 | 5.91     |
| Indeno[1,2,3- <i>cd</i> ]pyrene | IP           | 6               | 278                                   | 0.00019                               | 6.50     |
| Benzo[ <i>ghi</i> ]perylene     | B(ghi)P      | 6               | 276                                   | 0.00026                               | 6.50     |

### 2.3. Isolation and fractionation of the organic extract

The organic extractions of the samples were carried out on 3–9 g, according to the total organic carbon concentrations [20], with an automated accelerated solvent extractor (Dionex ASE 200) using dichloromethane (DCM), at 130 °C and 130 bars.

Copper powder, to eliminate the molecular sulfur; sodium sulfate, to remove the remaining molecules of water; and Fontainebleau sand, to increase the extraction yield, were added to the samples prior to the extraction. Then, the extracts were diluted with DCM to 20 mL and an aliquot was sampled and dried under nitrogen to determine the yield of the solvent extractable organic matter (EOM).

The fractionation into aliphatic, aromatic and polar families was performed on alumina and silica columns. Briefly, the aliphatic, aromatic and low molecular weight polar compounds were isolated from polar macromolecules on an alumina column, eluted successively with DCM and a mixture of DCM/methanol (1/1, v/v). The DCM fraction was then eluted on a silica column successively with *n*-heptane, a mixture of *n*-heptane/DCM (2/1, v/v), and a mixture of DCM/methanol (1/1, v/v), to recover respectively aliphatic hydrocarbons (HC), aromatic HC and polar fractions. The aromatic fractions,



containing the PAHs were then diluted to 5 mL with DCM and an aliquot was dried and weighed to determine the mass proportion of each fraction.

#### *2.4. PAH quantification*

An internal PAH standard mix ( $[^2\text{H}_8]$ naphthalene,  $[^2\text{H}_{10}]$ acenaphthene,  $[^2\text{H}_{10}]$ phenanthrene,  $[^2\text{H}_{12}]$ chrysene,  $[^2\text{H}_{12}]$ perylene, supplied by Cluzeau®) was added to the diluted aromatic fractions, before being injected in a GC–MS. The GC–MS was previously calibrated with mixtures of 16 PAHs listed by the US-EPA (naphthalene, acenaphthylene, acenaphthene, fluorene, phenanthrene, anthracene, fluoranthene, pyrene, benzo[a]anthracene, chrysene, benzo[b]fluoranthene, benzo[k]fluoranthene, benzo[a]pyrene, benzo[ghi]perylene, indeno[1,2,3-cd]pyrene, dibenzo[a,h]anthracene, supplied by Supelco). The GC used was a Hewlett Packard G1800A equipped with a capillary column in silica glass DB5-MS (60 m  $\times$  0.125 mm i.d.  $\times$  0.1  $\mu\text{m}$  film thickness) coupled to a MS Hewlett Packard GCD System detector on the fullscan mode. The temperature program was the following: from 70 °C to 130 °C at 15 °C  $\text{min}^{-1}$ , then from 130 °C to 315 °C at 3 °C  $\text{min}^{-1}$  and then a 15 min hold at 315 °C. The carrier gas was helium at 1.4 mL  $\text{min}^{-1}$  constant flow.

The 16 calibrated PAHs were quantified using the response factors obtained after the calibration. The concentrations of alk-PAHs were estimated using the response factors of the par-PAHs. The diagnostic ratios reported in Table 1 were then calculated for all the samples using the calculated PAH concentrations.

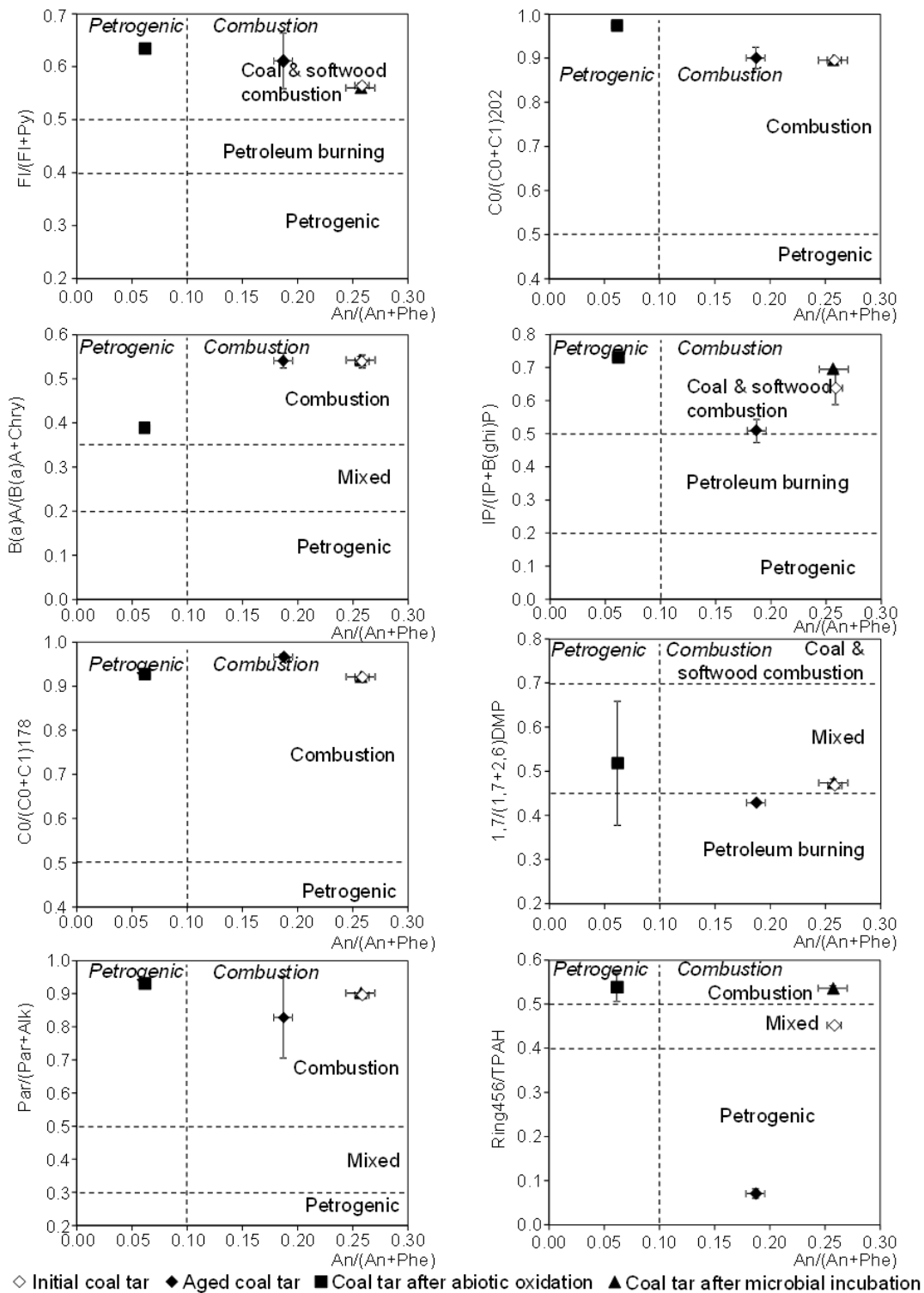


**Figure 1:** PAH diagnostic ratios presented in Table 1 of the coal tar sample, ◇ initial, ◆ “aged” coal tar from the Homecourt coking plant soil, ▲ coal tar after microbial incubation ■ coal tar after abiotic oxidation experiment. The bars represent the standard deviation.

### 3. Results and discussion

#### 3.1. PAH diagnostic ratios of the initial samples

Most of the PAH diagnostic ratio values of the initial coal tar samples exhibit the proper “coal combustion” or “coal and softwood combustion” signatures (Fig. 1). Only the 1,7-dimethylphenanthrene/(1,7-dimethylphenanthrene + 2,6-dimethylphenanthrene) ( $1,7/(1,7 + 2,6)\text{DMP}$ ) and the sum of the 4-, 5- and 6-ring PAHs/sum of the total PAHs (Ring 456/TPAH) ratios (Table 1) showed a mixed signature between petrogenic and combustion contributions. Coal tar is generated during production of coke or gas from the coal pyrolysis. This high temperature treatment can be assimilated to a combustion process [24,25]. However, contrary to other combustion products, such as soot or charred materials, the coal tar is enriched in low molecular weight PAHs [20,26,27]. That explains the relatively low Ring 456/TPAH ratio, plotting the coal tar sample in the mixed signature zone. The “aged” coal tar presents the same signatures as the fresh one, except for the  $1,7/(1,7 + 2,6)\text{DMP}$  and the 456 Ring/TPAH ratios for which it shows petroleum burning and petrogenic signatures, respectively.

About half of the calculated PAH diagnostic ratios are not representative of the petrogenic signature of the initial coal sample (Fig. 2). The values of the  $\text{B(a)A}/(\text{B(a)A} + \text{Chry})$  and  $1,7/(1,7 + 2,6)\text{DMP}$  ratios plotted the coal samples in the “combustion” and “coal and softwood combustion” zones, respectively, the  $\text{Indeno}[1,2,3\text{-cd}]\text{pyrene}/(\text{Indeno}[1,2,3\text{-cd}]\text{pyrene} + \text{Benzo}[\text{ghi}]\text{perylene})$  ( $\text{IP}/(\text{IP} + \text{B}(\text{ghi})\text{P})$ ) ratio exhibits a value corresponding to petroleum burning and the sample is plotted at the limit between combustion and mixed source for the Ring 456/TPAH ratio. Pies et al. [28] also found coal PAH diagnostic ratios with combustion and petroleum combustion signatures. Yunker et al. [11] and references therein reported an  $\text{Anthracene}/(\text{Anthracene} + \text{Phenanthrene})$  ( $\text{An}/(\text{An} + \text{Phe})$ ) ratio value of 0.20 for a coal sample, which corresponds to a combustion contribution. The  $\text{An}/(\text{An} + \text{Phe})$  and sum of An and Phe/sum of An, Phe and their methylated counterparts ( $\text{C0}/(\text{C0} + \text{C1})_{178}$ ) ratios, calculated from Zhao et al. [29] on high volatile and low volatile bituminous coal sample varied from 0 to 0.68 and

0 to 0.70, respectively, placing the highest values in the combustion zone. These wide ranges of PAH diagnostic ratios, observed for coal samples, can be explained by the different coal compositions according to their origin, ranks and coalification history [30]. For example, the degree of alkylation decreases with the increasing rank, and low molecular weight compounds (such as 2 and 3-ring PAHs) are generated during the formation of sub-bituminous to high volatile bituminous coals whereas the PAH distributions of high rank coals are dominated by 4 and more-ring PAHs [31]. Stout and Emsbo-Mattingly [32] determined PAH concentrations from different coal ranks (lignites, sub-bituminous coals, low volatile, medium volatile and high volatile bituminous coals, semi-anthracite and anthracite). The different ratios, presented in Table 1, (except the  $1,7/(1,7 + 2,6)\text{DMP}$  ratio) were calculated from the published data (Fig. 3). It appears that higher rank coals present a petrogenic signature for the  $\text{An}/(\text{An} + \text{Phe})$ ,  $\text{Fluoranthene}/(\text{Fluoranthene} + \text{Pyrene}) ((\text{Fl})/(\text{Fl} + \text{Py}))$  and  $\text{B(a)A}/(\text{B(a)A} + \text{Chry})$  ratios whereas low to medium rank coals present a mixed or combustion signature. On the contrary, higher rank coals show a combustion signature with the  $\text{C0}/(\text{C0} + \text{C1})_{178}$  and  $\text{sum of Fl and Py}/\text{sum of Fl, Py}$  and their methylated counterparts ( $\text{C0}/(\text{C0} + \text{C1})_{202}$ ) ratios whereas the calculated ratios of the other coal samples exhibited values consistent with a petrogenic signature. For the other calculated ratios there was no apparent connection between their values and the coal rank. From this brief review of the data available in the literature, it appears that the PAH diagnostic ratios defined for the petrogenic sources did not integrate a wide range of coal of different ranks and origins.

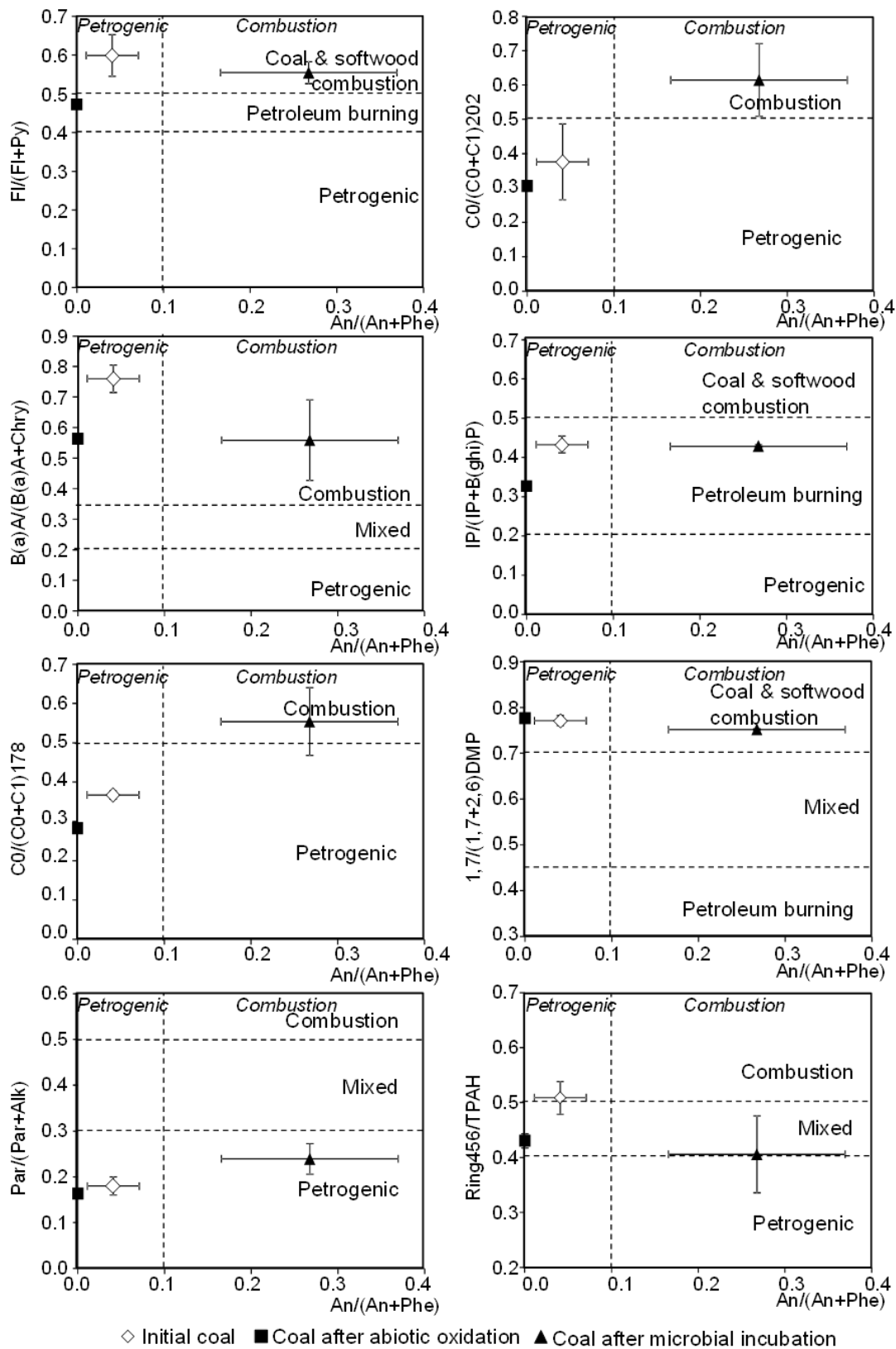


**Figure 2:** PAH diagnostic ratios presented in Table 2 of the coal sample, ◇ initial, ▲ after microbial incubation ■ after abiotic oxidation experiment. The bars represent the standard deviation.

Concerning the initial sample of the coking plant soil (Fig. 4), the ratios show a PAH origin mainly from “combustion” and “coal and softwood combustion”, except for the  $1,7/(1,7 + 2,6)$ DMP ratio which show a mixed source signature. The Ring 456/TPAH ratio indicates a petrogenic signature as it was also observed for the Ring 456/TPAH ratio of the coal tar. It is consistent with the fact that the main PAH contribution in coking plant soil is due to the abundance of coal tar. This fact was established by petrographic analysis which showed that the Homécourt coking plant soil contains 1.9% of coal tar and pitch [19]. The mixed signature, shown by the  $1,7/(1,7 + 2,6)$ DMP ratio, can be explained by the coal contribution. Indeed, this soil contains 7.4% of coal [19] and coal is particularly enriched in alk-PAHs [20]. Coal contribution in the soil was then expressed through this ratio, exclusively based on the dimethyl-phenanthrene concentrations.

### *3.2. Impact of the oxidation on the PAH diagnostic ratios*

The major change of signature of the oxidized coal tar is observed for the  $An/(An + Phe)$  ratio (Fig. 1). The ratio decreased from a combustion signature to a petrogenic signature. Lundstedt et al. [33] also observed higher degradation rate for anthracene compared to phenanthrene after an ethanol-Fenton treatment, which is basically a catalyzed oxidation reaction, on an aged gaswork soil. This change can be explained by the fact that anthracene is particularly sensitive to oxidation due to the presence of a preferential oxidation site on the carbons number 9 and 10 [34]. A decrease in the  $B(a)A/(B(a)A + Chry)$  ratio was also observed, leading to a shift of the plot toward the “mixed” zone. Kim et al. [18] also made the same observation after simulating the aging of soot particles by exposing them to irradiation. After photo-oxidation reactions the soot combustion signature changed to “petrogenic”. An increase in the  $C0/(C0 + C1)_{202}$  and Ring 456/TPAH ratios of was also observed. It preserved, for the first one, and shifted, for the latter, the signature to the combustion zone. The other ratios were conservative of the combustion signature of the coal tar sample. It is interesting to notice that the “aged” coal tar sample represents an intermediary between fresh coal tar and oxidized coal tar. If most of the ratio signatures were similar for the “aged” and the fresh coal tar, a trend toward the oxidized coal tar

signature is observed. The aging process, occurring naturally in the soil over a long period of time, was artificially reproduced and speeded up with the experimental abiotic oxidation, explaining the similar trends observed for both samples.

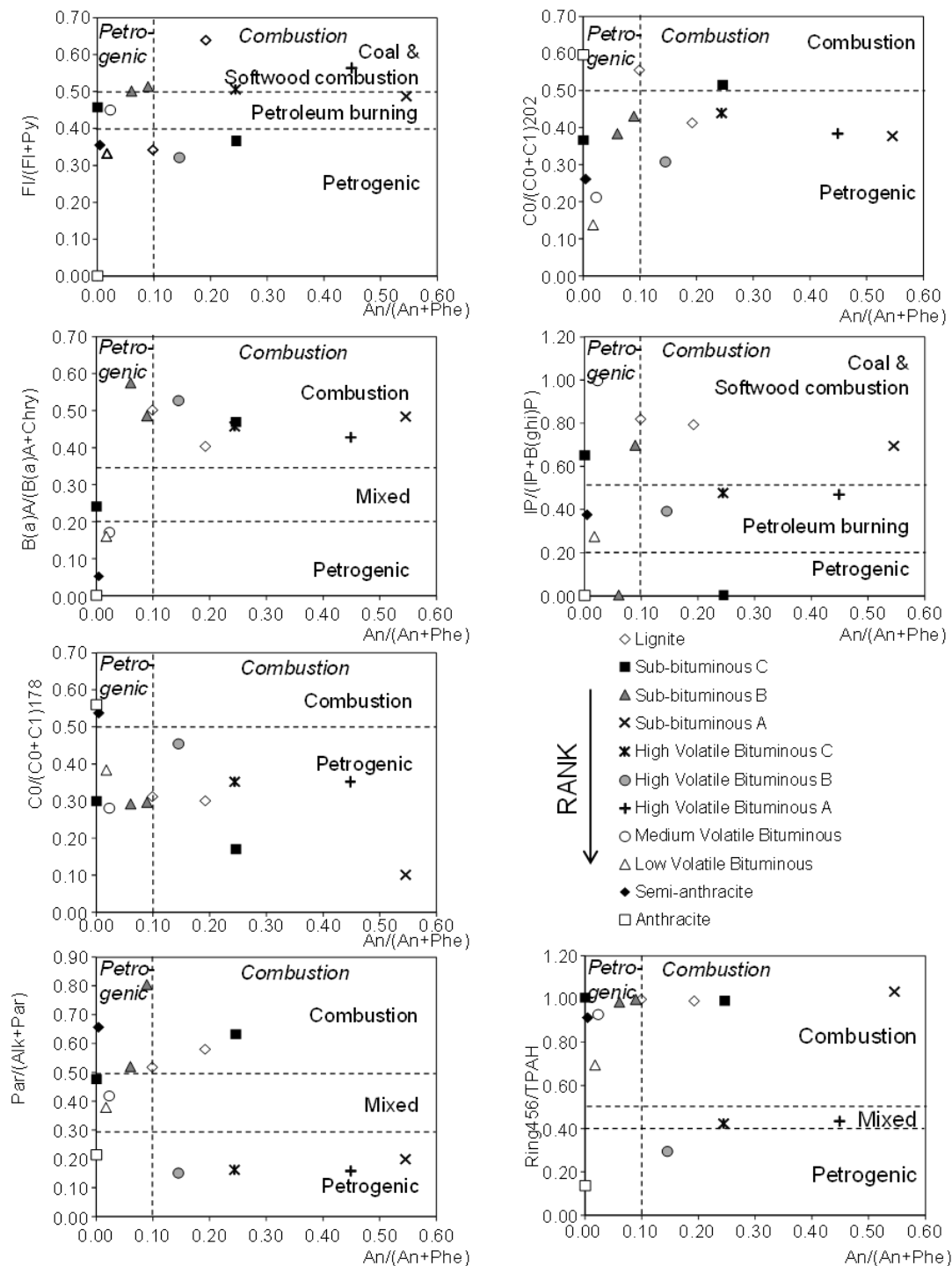


Figure 3: PAH diagnostic ratios for different coal ranks, calculated from Stout and Emsbo-Mattlingly [30].

The coal oxidation induced a complete degradation of anthracene, leading to a decrease in the  $An/(An + Phe)$  ratio to 0, which still corresponds to a petrogenic signature (Fig. 2). The  $Fl/(Fl + Py)$  and Ring 456/TPAH ratios decreased from “coal and softwood combustion” to “petroleum burning” signature and from “combustion” to “mixed” signature, respectively. A decrease in the  $B(a)A/(B(a)A + Chry)$ ,  $IP/(IP + B(ghi)P)$  and  $C0/(C0 + C1)_{178}$  diagnostic ratios was also observed but the initial ignatures (i.e., combustion, petroleum burning and petrogenic, respectively) remained unchanged.

As observed for the other samples, the oxidation of the coking plant soil induced a decrease in the  $An/(An + Phe)$  diagnostic ratio which did not affect the “combustion” signature of the sample (Fig. 4). An increase in the  $Fl/(Fl + Py)$ ,  $C0/(C0 + C1)_{178}$ ,  $C0/(C0 + C1)_{202}$  and sum of PAHs with  $m/z$  128, 178, 202 and 228/sum of these parent compounds and their alkylated counterparts ( $Par/(Alk + Par)$ ) ratios was observed but the combustion signature was preserved. As it was the case for the other samples, the  $B(a)A/(B(a)A + Chry)$  ratio decreased leading, this time, to a change of signature from a combustion origin to a mixed origin. The 456 Ring/TPAH ratio increased and the signature changed from a petrogenic contribution to a mixed contribution. Due to the absence of these compounds after the oxidation experiment of the coking plant soil, the  $1,7/(1,7 + 2,6)DMP$  ratio could not be calculated.

### *3.3. Impact of biodegradation on the PAH diagnostic ratios*

The biodegradation of coal induced a major change in the  $An/(An + Phe)$  ratio from a petrogenic to a combustion contribution (Fig. 2). Contrary to oxidation, phenanthrene is much more sensitive to biodegradation compared to anthracene. Moody et al. [35] observed higher degradation rate for phenanthrene, compared to anthracene, in the case of pure compound degradation by cell suspension of a *Mycobacterium* strain. Viñnas et al. [36] also observed higher proportion of removal for phenanthrene than for anthracene after bioremediation treatments of a creosote contaminated soil. This is due to phenanthrene higher solubility (Table 2) which makes it more bioavailable and, as a result, preferentially degraded compared to anthracene. The  $C0/(C0 + C1)_{178}$  and  $C0/(C0 + C1)_{202}$  ratios also changed from a petrogenic signature to a combustion contribution. This evolution was not



expected since alkylated compounds are more resistant to biodegradation than parent compounds [37–39]. However, as discussed in Biache et al. [19], the coal kerogen (i.e., the fraction of coal insoluble in organic solvents) is likely to produce lower molecular weight compounds by cracking occurring during biodegradation [40–42]. In fact, the variation of the ratios is not the consequence of a preferential degradation of alk-PAHs compared to par-PAHs but is caused by a slight decrease of the alk-PAH concentrations and mostly by an increase in the PAH concentrations [19]. These observations are consistent with the process of kerogen cracking during biodegradation and explain the variation of the latter ratios as well as the slight increase in the Par/(Par + Alk) ratio.

The biodegradation experiment seemed to be conservative on the PAH diagnostic ratios of the coal tar sample (Fig. 1). The only change observed was for the Ring 456/TPAH which increased. However it has been reported that the coal tar had a toxic effect on the inoculated microorganism during this experiment [19]. Consequently, the effect of biodegradation cannot be observed for this sample. It is likely that the change in the ratio Ring 456/TPAH is due to the volatilization of the low molecular weight PAHs.

As observed for the coal sample, the biodegradation of the coking plant soil induced an increase in the An/(An + Phe) ratio, but being plotted in the combustion zone it did not induce any change of the signature (Fig. 4). The Fl/(Fl + Py) ratio decreased after the biodegradation experiment and shifted the plot close to the petroleum burning area. The Par/(Par + Alk) ratio increased without inducing any change in the signature. The other diagnostic ratios of the biodegraded coking plant soil remained unchanged with a dominant “combustion” and “coal and softwood combustion” signature, except for the 1,7/(1,7 + 2,6)DMP and Ring 456/TPAH who kept their mixed and petrogenic signatures, respectively.

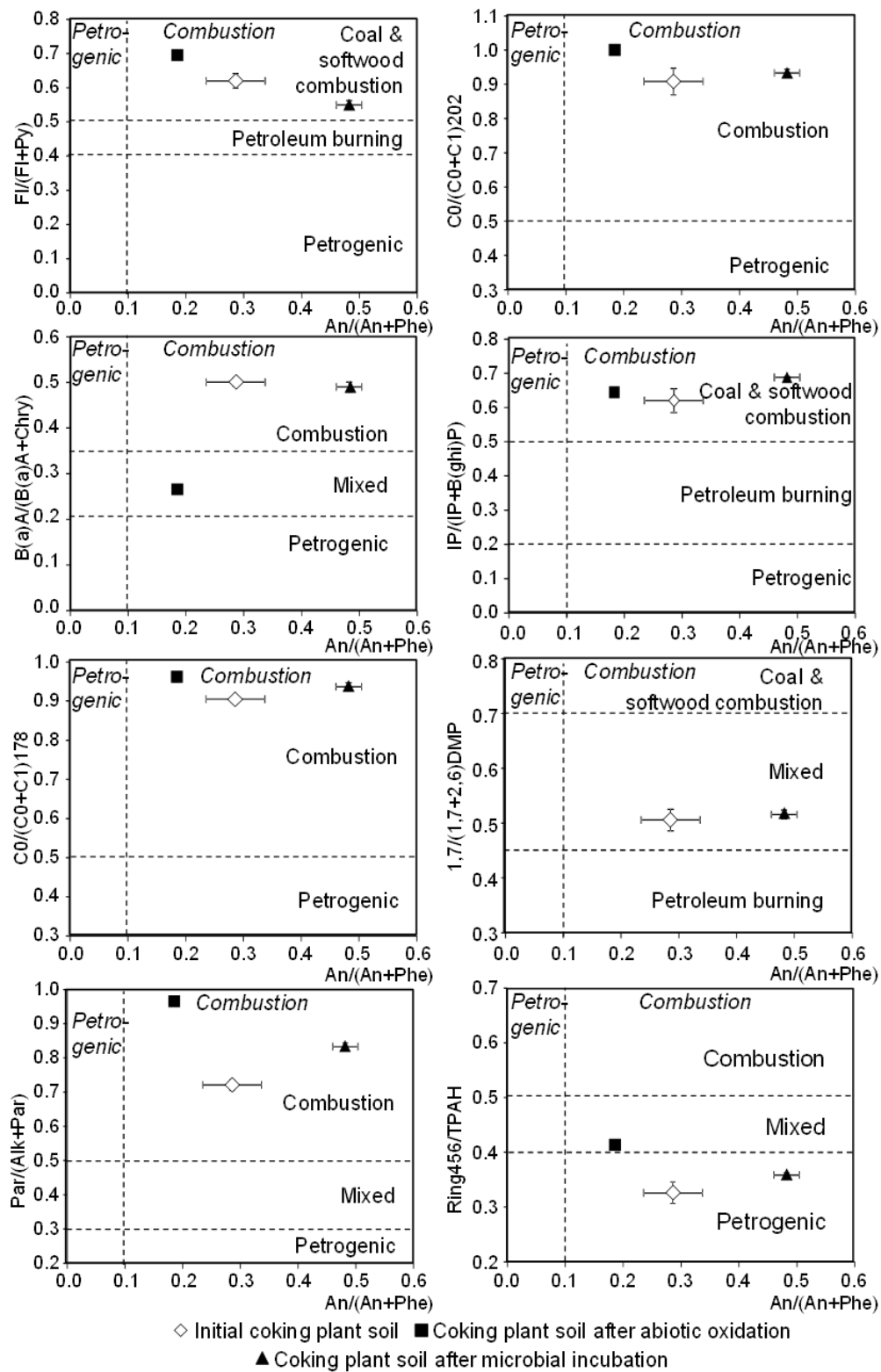


**Figure 4:** PAH diagnostic ratios presented in Table 2 of the coking plant soil sample, ◇ initial, ▲ after microbial incubation ■ after abiotic oxidation experiment. The bars represent the standard deviation.

#### 4. Conclusions

If the diagnostic ratios of the initial coal tar sample were consistent with the source signature (i.e., combustion) it was not the case of the initial coal sample for which only half of the calculated ratio designated the adequate petrogenic signature of the sample. The great variety of coal compositions, according to their origins and ranks, makes these PAH diagnostic ratios unsuitable to report the petrogenic origin of the coal. A mixed zone could be included or extended in order to incorporate the samples originated from different sources (i.e., petrogenic and combustion) and presenting the same ratio values.

The calculated ratios for the initial coking plant soil sample, exhibiting mostly a combustion signature, indicate the major contribution of coal tar in this sample. Considering the high PAH concentrations in coal tar, it is considered as a main source of PAHs in coking plant soil.

Due to the preferential transformation of some PAH isomers, the oxidation experiment and, in a lesser extent, the microbial incubation, induced some drastic modifications in the diagnostic ratios. These findings obtained from batch experiments show the modifications that the diagnostic ratios can undergo in field situation during natural attenuation, especially if the environmental conditions are favorable for one, or both studied processes.

As a result, and as underlined by several authors [28,43,44], caution must be taken while using these PAH diagnostic ratios as source indicators as they can be drastically modified by processes occurring during the transport and sequestration of the compounds. It is advised to calculate multiple ratios, and in particular ratios involving high molecular weight PAHs which seemed less sensitive to degradation, and to use other tools (such as the study of the aliphatic compound distribution or the use of petrography to identify particles of coal or coal tar for example) in order to confirm the origin of the PAHs.

## Acknowledgements

We thank the French “Ministère de l’Enseignement Supérieur et de la Recherche” (the French Ministry of Higher Education and Research) for financial support of this study as well as the GISFI (French Scientific Interest Group - Industrial Wasteland, [www.gisfi.prd.fr](http://www.gisfi.prd.fr)).

## References

- [1] C.A. Menzie, B.B. Potocki, J. Santodonato, Exposure to carcinogenic PAHs in the environment, *Environ. Sci. Technol.* 26 (1992) 1278–1284.
- [2] J.C. Means, Sorption of polynuclear aromatic hydrocarbons by sediments and soils, *Environ. Sci. Technol.* 14 (1980) 1524–1528.
- [3] M.J. Suess, The environmental load and cycle of polycyclic aromatic hydrocarbons, *Sci. Total Environ.* 6 (1976) 239–250.
- [4] G. Witt, Polycyclic aromatic hydrocarbons in water and sediment of the Baltic Sea, *Mar. Pollut. Bull.* 31 (1995) 237–248.
- [5] L.H. Keith, W.A. Telliard, Priority pollutants I – a perspective view, *Environ. Sci. Technol.* 13 (1979) 416–423.
- [6] M.B. Yunker, R.W. Macdonald, L.R. Snowdon, B.R. Fowler, Alkane and PAH biomarkers as tracers of terrigenous organic carbon in Arctic Ocean sediments, *Org. Geochem.* 42 (2011) 1109–1146.
- [7] J.C. Colombo, E. Pelletier, C. Brochu, M. Khalil, Determination of hydrocarbon sources using n-alkane and polyaromatic hydrocarbon distribution indexes. Case study: Rio de La Plata estuary, Argentina, *Environ. Sci. Technol.* 23 (1989) 888–894.

- [8] A. Katsoyiannis, E. Terzi, Q.-Y. Cai, On the use of PAH molecular diagnostic ratios in sewage sludge for the understanding of the PAH sources. Is this use appropriate? *Chemosphere* 69 (2007) 1337–1339.
- [9] B. Yan, T.A. Abrajano, R.F. Bopp, D.A. Chaky, L.A. Benedict, S.N. Chillrud, Molecular tracers of saturated and polycyclic aromatic hydrocarbon inputs into Central Park lake, New York City, *Environ. Sci. Technol.* 39 (2005) 7012–7019.
- [10] M.B. Yunker, R.W. Macdonald, Alkane and PAH depositional history, sources and fluxes in sediment from the Fraser River Basin and Strait of Georgia, Canada, *Org. Geochem.* 34 (2003) 1429–1454.
- [11] M.B. Yunker, R.W. Macdonald, R. Vingarzan, R.H. Mitchell, D. Goyette, S. Sylvestre, PAHs in the Fraser River basin: a critical appraisal of PAH ratios as indicators of PAH source and composition, *Org. Geochem.* 33 (2002) 489–515.
- [12] M.B. Yunker, L.R. Snowdon, R.W. Macdonald, J.N. Smith, M.G. Fowler, D.N. Skibo, F.A. McLaughlin, A.I. Danyushevskaya, V.I. Petrova, G.I. Ivanov, Polycyclic aromatic hydrocarbon composition and potential sources for sediment samples from the Beaufort and Barents seas, *Environ. Sci. Technol.* 30 (1996) 1310–1320.
- [13] X.L. Zhang, S. Tao, W.X. Liu, Y. Yang, Q. Zuo, S.Z. Liu, Source diagnostics of polycyclic aromatic hydrocarbons based on species ratios: a multimedia approach, *Environ. Sci. Technol.* 39 (2005) 9109–9114.
- [14] R.C. Brandli, T.D. Bucheli, S. Ammann, A. Desales, A. Keller, F. Blum, W.A. Stahel, Critical evaluation of PAH source apportionment tools using data from the Swiss soil monitoring network, *J. Environ. Monit.* 10 (2008) 1278–1286.

- [15] A. Katsoyiannis, A.J. Sweetman, K.C. Jones, PAH molecular diagnostic ratios applied to atmospheric sources: a critical evaluation using two decades of source inventory and air concentration data from the UK, *Environ. Sci. Technol.* 45 (2011) 8897–8906.
- [16] M. Tobiszewski, J. Namieśnik, PAH diagnostic ratios for the identification of pollution emission sources, *Environ. Pollut.* 162 (2012) 110–119.
- [17] A. Wagener, C. Hamacher, C. Farias, J.M. Godoy, A. Scofield, Evaluation of tools to identify hydrocarbon sources in recent and historical sediments of a tropical bay, *Mar. Chem.* 121 (2010) 67–79.
- [18] D. Kim, B.M. Kumfer, C. Anastasio, I.M. Kennedy, T.M. Young, Environmental aging of polycyclic aromatic hydrocarbons on soot and its effect on source identification, *Chemosphere* 76 (2009) 1075–1081.
- [19] C. Biache, P. Faure, L. Mansuy-Huault, A. Cébron, T. Beguiristain, C. Leyval, Biodegradation of the organic matter in a coking plant soil and its main constituents, *Org. Geochem.* 56 (2013) 10–18.
- [20] C. Biache, T. Ghislain, P. Faure, L. Mansuy-Huault, Low temperature oxidation of a coking plant soil organic matter and its major constituents: an experimental approach to simulate a long term evolution, *J. Hazard. Mater.* 188 (2011) 221–230.
- [21] C. Biache, L. Mansuy-Huault, P. Faure, C. Munier-Lamy, C. Leyval, Effects of thermal desorption on the composition of two coking plant soils: impact on solvent extractable organic compounds and metal bioavailability, *Environ. Pollut.* 156 (2008) 671–677.
- [22] C. Achten, S. Cheng, K.L. Straub, T. Hofmann, The lack of microbial degradation of polycyclic aromatic hydrocarbons from coal-rich soils, *Environ. Pollut.* 159 (2011) 623–629.
- [23] A. Regier, Détermination des sources de HAP dans les boues de station d'épuration lorraines (Determination of PAH sources in the sludge from Lorraine wastewater treatment plants), Agence de l'eau Rhin-Meuse (Rhin-Meuse Water Agency), 2005, 85 pp.

- [24] J.M. Costes, V. Druelle, Les hydrocarbures aromatiques polycycliques dans l'environnement: la réhabilitation des anciens sites industriels, [Polycyclic aromatic hydrocarbons in the environment: rehabilitation of former industrial sites], *Rev. I. Fr. Petrol.* 52 (1997) 425–440.
- [25] E. Mendonça, A. Picado, Ecotoxicological monitoring of remediation in a coke oven soil, *Environ. Toxicol.* 17 (2002) 74–79.
- [26] R.G. Luthy, D.A. Dzombak, C.A. Peters, S.B. Roy, A. Ramaswami, D. Nakles, B.R. Nott, Remediating tar-contaminated soils at manufactured gas plant sites, *Environ. Sci. Technol.* 28 (1994) 266A–276A.
- [27] S.A. Wise, B.A. Benner, G.D. Byrd, S.N. Chesler, R.E. Rebbert, M.M. Schantz, Determination of polycyclic aromatic hydrocarbons in a coal tar standard reference material, *Anal. Chem.* 60 (1988) 887–894.
- [28] C. Pies, B. Hoffmann, J. Petrowsky, Y. Yang, T.A. Ternes, T. Hofmann, Characterization and source identification of polycyclic aromatic hydrocarbons (PAHs) in river bank soils, *Chemosphere* 72 (2008) 1594–1601.
- [29] Z.-B. Zhao, K. Liu, W. Xie, W.-P. Pan, J.T. Riley, Soluble polycyclic aromatic hydrocarbons in raw coals, *J. Hazard. Mater.* 73 (2000) 77–85.
- [30] S. Laumann, V. Micić, M.A. Krüge, C. Achten, R.F. Sachsenhofer, J. Schwarzbauer, T. Hofmann, Variations in concentrations and compositions of polycyclic aromatic hydrocarbons (PAHs) in coals related to the coal rank and origin, *Environ. Pollut.* 159 (2011) 2690–2697.
- [31] C. Achten, T. Hofmann, Native polycyclic aromatic hydrocarbons (PAH) in coals – a hardly recognized source of environmental contamination, *Sci. Total Environ.* 407 (2009) 2461–2473.
- [32] S.A. Stout, S.D. Emsbo-Mattingly, Concentration and character of PAHs and other hydrocarbons in coals of varying rank – implications for environmental studies of soils and sediments containing particulate coal, *Org. Geochem.* 39 (2008) 801–819.

- [33] S. Lundstedt, Y. Persson, L. Öberg, Transformation of PAHs during ethanol- Fenton treatment of an aged gasworks' soil, *Chemosphere* 65 (2006) 1288–1294.
- [34] E. Perraudin, H. Budzinski, E. Villenave, Identification and quantification of ozonation products of anthracene and phenanthrene adsorbed on silica particles, *Atmos. Environ.* 41 (2007) 6005–6017.
- [35] J.D. Moody, J.P. Freeman, D.R. Doerge, C.E. Cerniglia, Degradation of phenanthrene and anthracene by cell suspensions of mycobacterium sp. strain PYR-1, *Appl. Environ. Microbiol.* 67 (2001) 1476–1483.
- [36] M. Viñas, J. Sabaté, M.J. Espuny, A.M. Solanas, Bacterial community dynamics and polycyclic aromatic hydrocarbons degradation during bioremediation of heavily creosote-contaminated soil, *Appl. Environ. Microbiol.* 71 (2005) 7008–7018.
- [37] M. Ahmed, J.W. Smith, S.C. George, Effects of biodegradation on Australian Permian coals, *Org. Geochem.* 30 (1999) 1311–1322.
- [38] H. Huang, B.F.J. Bowler, T.B.P. Oldenburg, S.R. Larter, The effect of biodegradation on polycyclic aromatic hydrocarbons in reservoir oils from the Liaohe basin, NE China, *Chemosphere* 35 (2004) 1619–1634.
- [39] J.K. Volkman, R. Alexander, R.I. Kagi, S.J. Rowland, P.N. Sheppard, Biodegradation of aromatic hydrocarbons in crude oils from the barrow Sub-basin of Western Australia, *Org. Geochem.* 6 (1984) 619–632.
- [40] M. Hofrichter, D. Ziegenhagen, S. Sorge, R. Ullrich, F. Bublitz, W. Fritsche, Degradation of lignite (low-rank coal) by lignolytic basidiomycetes and their manganese peroxidase system, *Appl. Microbiol. Biotechnol.* 52 (1999) 78–84.
- [41] H. Machnikowska, K. Pawelec, A. Podgórska, Microbial degradation of low rank coals, *Fuel Process. Technol.* 77–78 (2002) 17–23.



- [42] G. Wadhwa, D.K. Sharma, Microbial pretreatments of coals: a tool for solubilization of lignite in organic solvent – quinoline, *World J. Microb. Biotechnol.* 14 (1998) 751–763.
- [43] L. Jeanneau, P. Faure, E. Montarges-Pelletier, M. Ramelli, Impact of a highly contaminated river on a more important hydrologic system: changes in organic markers, *Sci. Total Environ.* 372 (2006) 183–192.
- [44] L. Mansuy-Huault, A. Regier, P. Faure, Analyzing hydrocarbons in sewer to help in PAH source apportionment in sewage sludges, *Chemosphere* 75 (2009) 995–1002.

## Supplementary Data

Impact of oxidation and biodegradation on the most commonly used polycyclic aromatic hydrocarbon (PAH) diagnostic ratios: Implications for the source identifications

*Coralie Biache<sup>1,2\*</sup>, Laurence Mansuy-Huault<sup>1,2</sup>, Pierre Faure<sup>1,2</sup>*

<sup>1</sup> University of Lorraine, LIEC, UMR7360, Vandœuvre-lès-Nancy, F-54506, France

<sup>2</sup> CNRS, LIEC, UMR7360, Vandœuvre-lès-Nancy, F-54506, France

Table S1 : 16 PAH concentrations the sample after the abiotic experiments (nd = not detected)

|                         | Coal                                     |   | Coal-tar                                 |   | Coking plant soil                        |   |
|-------------------------|--|---|--|---|--|---|
|                         | T0 ( $\mu\text{g}\cdot\text{g}^{-1}$ dw) | T180d ( $\mu\text{g}\cdot\text{g}^{-1}$ dw) | T0 ( $\mu\text{g}\cdot\text{g}^{-1}$ dw) | T180d ( $\mu\text{g}\cdot\text{g}^{-1}$ dw) | T0 ( $\mu\text{g}\cdot\text{g}^{-1}$ dw) | T180d ( $\mu\text{g}\cdot\text{g}^{-1}$ dw) |
| Naphthalene             | 39 ± 22                                  | 24 ± 1                                      | 976 ± 149                                | 614 ± 146                                   | 5 ± 3                                    | nd  |
| Acenaphthylene          | nd                                       | nd  | 757 ± 54                                 | 18 ± 5                                      | 207 ± 33                                 | 108 ± 14                                    |
| Acenaphthene            | nd                                       | nd  | 23 ± 3                                   | nd  | 190 ± 44                                 | nd  |
| Fluorene                | 9 ± 3                                    | nd  | 562 ± 26                                 | nd  | 159 ± 16                                 | 17 ± 1                                      |
| Phenanthrene            | 42 ± 6                                   | 17 ± 2                                      | 1662 ± 178                               | 1256 ± 184                                  | 327 ± 42                                 | 235 ± 25                                    |
| Anthracene              | 2 ± 1                                    | nd  | 581 ± 83                                 | 83 ± 19                                     | 131 ± 28                                 | 53 ± 8                                      |
| Fluoranthene            | 5 ± 1                                    | 2 ± 0                                       | 1135 ± 136                               | 881 ± 132                                   | 148 ± 19                                 | 91 ± 5                                      |
| Pyrene                  | 4 ± 1                                    | 2 ± 0                                       | 877 ± 112                                | 509 ± 82                                    | 91 ± 14                                  | 40 ± 4                                      |
| Benzo(a)anthracene      | 11 ± 2                                   | 3 ± 0                                       | 356 ± 46                                 | 157 ± 28                                    | 49 ± 7                                   | 13 ± 2                                      |
| Chrysene                | 11 ± 2                                   | 4 ± 1                                       | 303 ± 21                                 | 246 ± 39                                    | 49 ± 6                                   | 36 ± 4                                      |
| Benzo(b)fluoranthene    | 9 ± 2                                    | 6 ± 0                                       | 286 ± 22                                 | 217 ± 40                                    | 45 ± 9                                   | 37 ± 3                                      |
| Benzo(k)fluoranthene    | 5 ± 2                                    | 3 ± 0                                       | 115 ± 7                                  | 83 ± 13                                     | 19 ± 3                                   | 13 ± 1                                      |
| Benzo(a)pyrene          | 11 ± 2                                   | 6 ± 0                                       | 298 ± 38                                 | 18 ± 4                                      | 37 ± 5                                   | 9 ± 1                                       |
| Indeno(1,2,3-c,d)pyrene | 11 ± 4                                   | 2 ± 0                                       | 271 ± 43                                 | 168 ± 33                                    | 37 ± 7                                   | 28 ± 3                                      |
| Benzo(g,h,i)perylene    | 14 ± 4                                   | 4 ± 0                                       | 153 ± 11                                 | 62 ± 11                                     | 23 ± 3                                   | 16 ± 1                                      |
| Dibenzo(a,h)anthracene  | 15 ± 6                                   | nd  | 42 ± 2                                   | 27 ± 4                                      | 13 ± 4                                   | 8 ± 0                                       |

Table S2 : 16 PAH concentrations after microbial incubation (nd = not detected)

|                        | Coal                          |                                     | Coal tar                      |                                     | Coking plant soil             |                                     |
|------------------------|-------------------------------|-------------------------------------|-------------------------------|-------------------------------------|-------------------------------|-------------------------------------|
|                        | T0 ( $\mu\text{g g}^{-1}$ dw) | 9 months ( $\mu\text{g g}^{-1}$ dw) | T0 ( $\mu\text{g g}^{-1}$ dw) | 9 months ( $\mu\text{g g}^{-1}$ dw) | T0 ( $\mu\text{g g}^{-1}$ dw) | 9 months ( $\mu\text{g g}^{-1}$ dw) |
| Naphthalene            | 39 $\pm$ 22                   | 41 $\pm$ 2                          | 976 $\pm$ 149                 | n.d.                                | 5 $\pm$ 3                     | 3 $\pm$ 2                           |
| Acenaphthylene         | nd                            | nd                                  | 757 $\pm$ 54                  | 331 $\pm$ 100                       | 207 $\pm$ 33                  | 188 $\pm$ 28                        |
| Acenaphthene           | nd                            | nd                                  | 23 $\pm$ 3                    | n.d.                                | 190 $\pm$ 44                  | 44 $\pm$ 6                          |
| Fluorene               | 9 $\pm$ 3                     | 7 $\pm$ 1                           | 562 $\pm$ 26                  | 386 $\pm$ 93                        | 159 $\pm$ 16                  | 63 $\pm$ 9                          |
| Phenanthrene           | 42 $\pm$ 6                    | 62 $\pm$ 14                         | 1662 $\pm$ 178                | 1460 $\pm$ 350                      | 327 $\pm$ 42                  | 124 $\pm$ 18                        |
| Anthracene             | 2 $\pm$ 1                     | 25 $\pm$ 15                         | 581 $\pm$ 83                  | 511 $\pm$ 150                       | 131 $\pm$ 28                  | 115 $\pm$ 11                        |
| Fluoranthene           | 5 $\pm$ 1                     | 9 $\pm$ 4                           | 1135 $\pm$ 136                | 975 $\pm$ 240                       | 148 $\pm$ 19                  | 58 $\pm$ 8                          |
| Pyrene                 | 4 $\pm$ 1                     | 7 $\pm$ 4                           | 877 $\pm$ 112                 | 768 $\pm$ 210                       | 91 $\pm$ 14                   | 48 $\pm$ 4                          |
| Benz[a]anthracene      | 11 $\pm$ 2                    | 9 $\pm$ 0                           | 356 $\pm$ 46                  | 298 $\pm$ 87                        | 49 $\pm$ 7                    | 28 $\pm$ 5                          |
| Chrysene               | 11 $\pm$ 2                    | 9 $\pm$ 0                           | 303 $\pm$ 21                  | 254 $\pm$ 82                        | 49 $\pm$ 6                    | 29 $\pm$ 5                          |
| Benzo[b]fluoranthene   | 9 $\pm$ 2                     | 7 $\pm$ 1                           | 286 $\pm$ 22                  | 185 $\pm$ 47                        | 45 $\pm$ 9                    | 31 $\pm$ 5                          |
| Benzo[k]fluoranthene   | 5 $\pm$ 2                     | 5 $\pm$ 1                           | 115 $\pm$ 7                   | 74 $\pm$ 20                         | 19 $\pm$ 3                    | 13 $\pm$ 2                          |
| Benz[a]pyrene          | 11 $\pm$ 2                    | 9 $\pm$ 1                           | 298 $\pm$ 38                  | 254 $\pm$ 66                        | 37 $\pm$ 5                    | 30 $\pm$ 5                          |
| Indeno[1,2,3-cd]pyrene | 11 $\pm$ 4                    | 11 $\pm$ 2                          | 271 $\pm$ 43                  | 234 $\pm$ 61                        | 37 $\pm$ 7                    | 37 $\pm$ 6                          |
| Benzo[ghi]perylene     | 14 $\pm$ 4                    | 14 $\pm$ 2                          | 153 $\pm$ 11                  | 103 $\pm$ 27                        | 23 $\pm$ 3                    | 17 $\pm$ 2                          |
| Dibenz[a,h]anthracene  | 15 $\pm$ 6                    | 15 $\pm$ 2                          | 42 $\pm$ 2                    | 28 $\pm$ 8                          | 13 $\pm$ 4                    | 11 $\pm$ 1                          |